

Fischer–Tropsch Kinetic Studies with Cobalt–Manganese Oxide Catalysts

Martin J. Keyser,[†] Raymond C. Everson,* and Rafael L. Espinoza[†]

School of Chemical and Minerals Engineering, Potchefstroom University for Christian Higher Education, Private Bag X6001, Potchefstroom 2520, South Africa

An investigation was undertaken to establish the reaction mechanism for the Fischer–Tropsch reaction, in the presence of the water–gas shift reaction, over a cobalt–manganese oxide catalyst under conditions favoring the formation of gaseous, liquid, and solid (waxes) hydrocarbons (210–250 °C and 6–26 bar). A micro-fixed-bed reactor was used with a cobalt–manganese oxide catalyst prepared by a coprecipitation method. An integral reactor model involving both Fischer–Tropsch and water–gas shift reaction kinetics was used to describe the overall performance. Reaction rate equations based on Langmuir–Hinshelwood–Hougen–Watson models for the Fischer–Tropsch reaction (hydrocarbon forming) and empirical reaction rate equations for the water–gas shift reaction from the literature were tested. Different combinations of the reaction rate equation were evaluated with the aid of a nonlinear regression procedure. It was found that a reaction rate equation for the Fischer–Tropsch reaction based on the enolic theory performed slightly better than a reaction rate equation based on the carbide theory. Reaction rate constants for the cobalt–manganese oxide catalyst are reported, and it is concluded that this catalyst also behaves very much like iron-based catalysts.

1. Introduction

The kinetics of the Fischer–Tropsch reaction with cobalt-based catalysts has been studied by many investigators (Anderson, 1956; Yang et al., 1979; Rautavuoma and Van der Baan, 1981; Sarup and Wojciechowski, 1989; Yates and Satterfield, 1991; Iglesia et al., 1993; Chanenchuk et al., 1991), and it has been shown that cobalt-based catalysts, in general, are superior to similarly prepared iron-based catalysts with respect to especially catalyst life. A well-known property of a cobalt-based catalyst is that it has no water–gas shift activity, under conditions favoring the Fischer–Tropsch reaction, which is in contrast to the behavior of iron-based Fischer–Tropsch catalysts. The suitability of a cobalt–manganese oxide catalyst (spinel form) for the Fischer–Tropsch process to produce gaseous, liquid, and solid (waxes) hydrocarbons was examined in our laboratories, and results have been published (Keyser et al., 1998). In contrast to other cobalt-based catalysts, this catalyst has significant water–gas shift activity in the presence of Fischer–Tropsch reactions at 21 bar pressure and 220 °C.

Intrinsic reaction rate equations for the Fischer–Tropsch equation (hydrocarbon forming only) based on the Langmuir–Hinshelwood–Hougen–Watson (LHHW) adsorption theory have been developed and used successfully for cobalt- and iron-based catalysts (Anderson, 1956; Rautavuoma and Van der Baan, 1981; Sarup and Wojciechowski, 1989; Yates and Satterfield, 1991; Attwood and Bennett, 1979; Huff and Satterfield, 1984; Nettelhoff et al., 1985; Dry, 1976; Ledakowicz et al., 1985; Lox and Froment, 1993). The mechanisms proposed include the carbide, enolic, and direct insertion theories.

The reaction rate of carbon monoxide conversion to carbon dioxide according to the water–gas shift over different catalysts with no Fischer–Tropsch activity, either because of the catalyst properties or under conditions not favoring the Fischer–Tropsch reaction, is well-known (Moe, 1962; Bohlbro, 1964; Ruthven, 1969; Newsome, 1980; Singh and Saraf, 1977; Oki and Mezaki, 1973a,b; Deluzarche et al., 1982; Grenoble et al., 1981). Two mechanistic models based on oxidation–reduction reactions and the presence of a formate species as a reactive intermediate have received special attention. An empirical reaction rate equation most frequently referred to in the literature is first order with respect to carbon monoxide concentration or partial pressure and has been used successfully. This equation, together with corrective terms to account for effects such as pressure, catalyst age, H₂S concentration, and diffusion, was used by Singh and Saraf (1977), Ruthven (1969), and others.

The reaction rate kinetics of the Fischer–Tropsch reaction over iron-based catalysts with the inclusion of the water–gas shift reaction has been examined in detail by Lox and Froment (1993) and Zimmerman and Bukur (1990). Huff and Satterfield (1984) and Dry (1976) also discussed the inclusion of the water–gas shift reaction but did not provide a detailed analysis thereof. All of these authors considered the synthesis to consist of a set of simultaneous series–parallel reactions involving the Fischer–Tropsch reactions (hydrocarbon forming) and the water–gas shift reaction (carbon dioxide forming). Lox and Froment (1993) using LHHW kinetics (elementary reactions) assumed the carbide mechanism for the hydrocarbon synthesis (Fischer–Tropsch reactions) and a theory based on a formate surface intermediate for the water–gas shift reaction. They evaluated models with results from a fixed-bed reactor and used the Schultz–Flory distribution to characterize the composition of the hydrocarbons.

* To whom correspondence should be addressed.

[†] Present address: Sastech Research and Development Division, P.O. Box 1, Sasolburg 9570, South Africa.

Model discrimination and parameter estimation was carried out with the aid of a regression procedure. Zimmerman and Bukur (1990) evaluated reaction rate equations for the Fischer–Tropsch reactions (lumped) and the water–gas shift reaction with results obtained from a slurry reactor with two different iron-based catalysts. Using existing reaction rate equations for the Fischer–Tropsch reaction, together with derived empirical equations for the water–gas shift reaction, they determined which equations (combination) best described the experimental results obtained. Parameter estimation and model discrimination were also done by regression.

An investigation was undertaken to elucidate the reaction kinetics of the cobalt–manganese oxide catalysts used by Keyser et al. (1998) and to compare its performance with other cobalt- and iron-based catalysts. For this purpose reaction rate equations based on fundamental principles (LHHW kinetics), for the hydrocarbon-forming reaction (Fischer–Tropsch) only, were evaluated. The presence of the water–gas shift reaction was accounted for by using a model consisting of a set of series–parallel reactions, also used by Zimmerman and Bukur (1990) and Lox and Froment (1993) with an empirical reaction rate equation for the water–gas shift reaction. Existing reaction rate equations from the literature were used together with an appropriate regression technique to discriminate between the models and to estimate the constants. The results presented in this paper consist of the following: (1) Evaluation of a suitable combination of reaction rate equations for the simultaneous Fischer–Tropsch and water–gas shift reactions. The Fischer–Tropsch reaction rates examined are all mechanistic-based equations and were carefully selected to include different surface reaction mechanisms. (2) Evaluation of reaction rate constants for the most suitable combination of reaction rates.

2. Experimental Section

2.1. Micro-Fixed-Bed Reactor. The reactor consisted of a single stainless steel tube with a diameter of 15 mm surrounded by an aluminum jacket to achieve a uniform wall temperature along the length of the reactor. A preheating zone ahead of the catalyst packing was filled with inert quartz glass beads. External heating was provided by an electrical element wrapped around the aluminum jacket. A schematic representation of the reactor is shown in Figure 1.

Pressures between 6 and 26 bar, temperatures between 210 and 250 °C, and hydrogen–carbon monoxide ratios of 1.65, 1.90, and 4.05 were used for the evaluation of the reaction rate equations.

2.2. Materials Used. The catalyst was prepared by coprecipitation, involving dissolved nitrate salts of cobalt and manganese in water, with ammonium hydroxide in a continuous precipitator similar to that described by Deckwer et al. (1982). The precipitate was filtered, washed, dried, mixed with gum acacia (Arabic gum), and extruded. The extrudates were calcined at 500 °C in the presence of nitrogen and were free of gum acacia. This study was carried out with a catalyst with a composition $\text{Co}/(\text{Co} + \text{Mn}) = 0.25$ (mass ratio) and had a BET surface area of 4.3 m²/g. A temperature-programmed reduction (TPR) determination showed reduction peaks at 230, 320, and 460 °C. The catalyst was analyzed by X-ray diffraction after reduction at 350 °C, and a mixed oxide

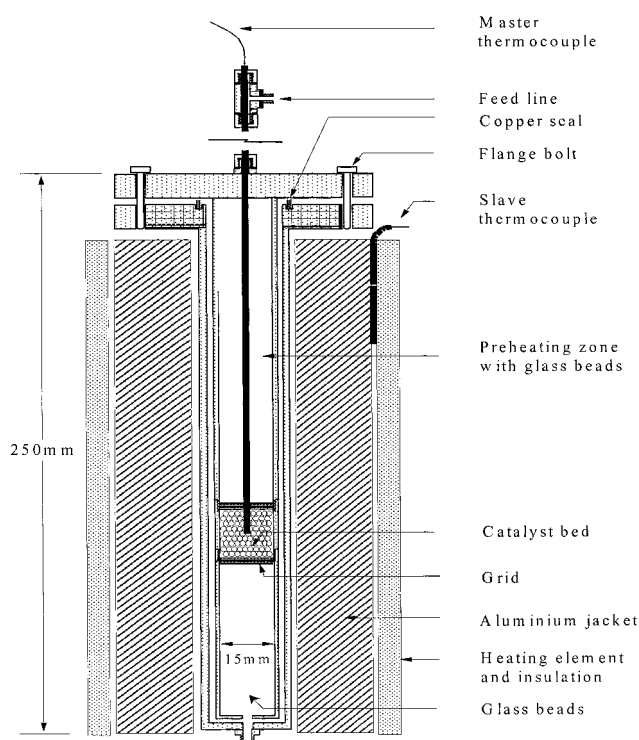


Figure 1. Micro-fixed-bed reactor.

spinel structure $(\text{CoMn})(\text{CoMn})_2\text{O}_4$ was identified (Keyser et al., 1998).

The gases used were of high purity supplied from prepared high-pressure gas cylinders with the necessary flow measurement and pressure adjustment. The chemicals for the catalyst preparation were of A.R. grade and were obtained from Merck Chemicals.

2.3. Procedure and Analysis. Experiments were performed with catalyst particles with a diameter between 1.0 and 1.5 mm and were prepared by crushing the extrudes. The catalyst loading with a mass of 6 g was reduced at atmospheric pressure and 350 °C in pure hydrogen for 16 h with a volumetric flow rate of 12 mL/min (STP). After reduction the reactor temperature was lowered to 150 °C, the synthesis gas introduced, and the pressure increased to the required reaction pressure. The reaction temperature was increased to 190 °C at a rate of 10 °C/h and was left overnight at 190 °C (± 16 h). The temperature was then increased from 190 °C to the reaction temperature at a rate of 5 °C/h. This procedure was adopted to ensure stable operation. Analysis of the products was carried out with a Chrompack 5000 gas chromatograph equipped with the appropriate columns and detectors in a carefully designed network of piping with an on-line multiport sample valve (Keyser, 1997).

3. Modeling and Evaluation

3.1. Reactor Model. An integral reactor model was used to describe the operation of the micro-fixed-bed reactor. The heat transfer in this reactor was also such that the catalyst packing was essentially isothermal for the operating conditions used. The effects of axial dispersion, interphase and intraparticle mass transport, and pressure drop were examined with well-established criteria (Everson et al., 1996; Mears, 1971; Finlayson, 1971; Young and Finlayson, 1973; Froment and Bischoff, 1990), and it was found that all of these effects

Table 1. Fischer–Tropsch Reaction Rates (LHHW Based)

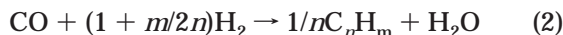
reference [also used to identify equation in text]	reaction rate	catalyst
Anderson ¹ (1956)	$r_{\text{FT}} = \frac{k_{\text{FT}} p_{\text{CO}} p_{\text{H}_2}^2}{1 + b p_{\text{CO}} p_{\text{H}_2}^2}$	Co/ThO ₂ /kieselguhr
Rautavuoma and Van der Baan (1981)	$r_{\text{FT}} = \frac{k_{\text{FT}} p_{\text{CO}}^{1/2} p_{\text{H}_2}}{(1 + b p_{\text{CO}}^{1/2})^3}$	Co/Al ₂ O ₃
Sarup and Wojciechowski (1989)	$r_{\text{FT}} = \frac{k_{\text{FT}} p_{\text{CO}}^{1/2} p_{\text{H}_2}^{1/2}}{(1 + b p_{\text{CO}}^{1/2} + c p_{\text{H}_2}^{1/2})^2}$	Co/kieselguhr
Yates and Satterfield (1991)	$r_{\text{FT}} = \frac{k_{\text{FT}} p_{\text{CO}} p_{\text{H}_2}}{(1 + b p_{\text{CO}})^2}$	Co/Mo/SiO ₂
Huff and Satterfield (1984)	$r_{\text{FT}} = \frac{k_{\text{FT}} p_{\text{CO}} p_{\text{H}_2}^2}{(p_{\text{H}_2\text{O}} + b p_{\text{CO}} p_{\text{H}_2})}$	fused Fe
Ledakowicz et al. (1985)	$r_{\text{FT}} = \frac{k_{\text{FT}} p_{\text{CO}} p_{\text{H}_2}}{(p_{\text{CO}} + b p_{\text{H}_2\text{O}} + c p_{\text{CO}_2})}$	precipitated Fe/K
Anderson ² (1956) Dry (1976) Attwood and Bennett (1979) Nettlehoff et al. (1985)	$r_{\text{FT}} = \frac{k_{\text{FT}} p_{\text{CO}} p_{\text{H}_2}}{(p_{\text{CO}} + b p_{\text{H}_2\text{O}})}$	reduced and nitrated Fe fused Fe nitrated fused Fe precipitated Fe

can be neglected. It was accordingly deduced that an isothermal one-dimensional pseudohomogeneous model with plug flow was applicable. The equations describing this model consist of a mass balance for each particular component which may be written as follows:

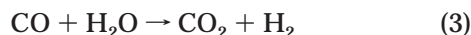
$$\frac{d(uc_i)}{dz} + r_i \rho_B = 0 \quad (1)$$

with the boundary condition $c_i = c_i^\circ$ at the reactor entrance ($z = 0$), c_i the concentration of component i (mol/m³), u the superficial velocity (m/s), r_i the overall reaction rate of component i [mol/(kg_{cat} s)], and ρ_B the catalyst bed density (kg_{cat}/m³). The catalyst used produced hydrocarbons with a broad spectrum of carbon numbers which were very difficult to measure accurately. To overcome this problem, a single representative chemical reaction involving average values, also used by other investigators (Zimmerman and Bukur, 1990; Blanks, 1992), was considered. With this approximation the overall synthesis (including the water–gas shift reaction) consisted of the following:

Fischer–Tropsch (FT)



water–gas shift (WGS)



where n is the average carbon chain length of the hydrocarbon product and m is the average number of hydrogen atoms per hydrocarbon molecule. For this particular study n and m were very close to values of 5 and 12, respectively; similar to that found by Blanks (1992). The overall reaction rate for each component (H₂, CO, CO₂, H₂O, and C_{*n*}H_{*m*}) consisted of the sum of the reaction rates of each chemical reaction (eqs 2 and 3) with the relevant stoichiometric coefficient; for example, $r_{\text{co}} = r_{\text{FT}} + r_{\text{WGS}}$ with r_{co} the total rate of consumption of carbon monoxide and r_{FT} and r_{WGS} the reaction rates of the reactions given by eqs 2 and 3, respectively.

3.2. Reaction Rate Equations. The reaction rate equations (r_{FT}) used for the Fischer–Tropsch reaction

(hydrocarbon forming) were all mechanistic-based equations taken from the literature. These equations are given in Table 1 together with the catalysts tested.

A characteristic of the cobalt-based catalyst in contrast to the iron-based catalyst is the absence of terms accounting for the effects of water and carbon dioxide. Also the rate equations applicable to the iron-based catalyst are such that the denominator contains terms which are much larger than unity, with the consequence that the denominator is simplified to the forms given in Table 1 (without unity), whereas the cobalt-based equations include a unity term.

For the catalyst used in this study, it was assumed that the Fischer–Tropsch and water–gas shift reactions occur on different active sites with no interaction between the respective surface reactions. For this purpose water–gas shift reaction rates (r_{WGS}) were selected from the literature which were developed for reaction systems with no Fischer–Tropsch activity. Reaction rates for cobalt-based catalysts have been examined and reported by Newsome (1980) and Overstreet (1974). Overstreet (1974) showed that a first-order rate equation in carbon monoxide was valid for a sulfided cobalt–manganese–cesium catalyst. Hutchings et al. (1992) observed water–gas shift activity with a cobalt–manganese oxide catalyst similar to that used in this study but was unable to evaluate a suitable reaction rate equation. The rate equation of Overstreet (1974) is the same as that used by Singh and Saraf (1977) for an iron-based catalyst and was used in the form proposed by Singh and Saraf (1977) in this investigation. A second-order equation involving carbon monoxide and water also used by Moe (1962) for an iron-based catalyst was also evaluated. These equations are given in Table 2 with the inclusion of a corrective term to account for the effect of total pressure according to Singh and Saraf (1977).

3.3. Evaluation of the Model with Reaction Rates. The reactor model (eq 1) with combinations of the different reaction rate equations (Tables 1 and 2) was solved numerically using backward differences for the discretization. An IMSL (version 9) nonlinear regression algorithm of Levenburg and Marquard (Brown and Dennis, 1972) was used to fit the models to the

Table 2. Water–Gas Shift Reaction Rates (Empirical)

reference [also used to identify equation in text]	reaction rate
Moe (1962)	$r_{\text{WGS}} = k_{\text{WGS}} \left(p_{\text{CO}} p_{\text{H}_2\text{O}} - \frac{p_{\text{H}_2} p_{\text{CO}_2}}{K_{\text{WGS}}} \right)$
Singh and Saraf (1977) (with pressure factor)	$r_{\text{WGS}} = k_{\text{WGS}} P_A (y_{\text{CO}} - y_{\text{CO}}^*)$ $r_{\text{WGS}} = k_{\text{WGS}} P \left(p_{\text{CO}} - \frac{p_{\text{H}_2} p_{\text{CO}_2}}{K_{\text{WGS}} p_{\text{H}_2\text{O}}} \right)$

experimental results and to estimate the reaction rate constants (Keyser, 1997).

The residual sum of squares (SSQ) was minimized for the calculation

$$\text{SSQ} = \sum_{j=1}^N \sum_{i=1}^M ((\hat{x}_{ij} - x_{ij})/x_{ij})^2 \quad (4)$$

where M is the number of experiments and N the number of chemical components, with \hat{x}_{ij} and x_{ij} the calculated and experimental variables.

A measure of the goodness of fit of the solution of the model with experimental results was assessed by the F -test using tabulated values for a 95% confidence interval, similar to the procedure used by Sarup and Wojciechowski (1989). For this purpose a parameter R is defined (Draper and Smith, 1990) as

$$R = (\text{SSQ}(\hat{\theta}) - \sigma^2 f)/(M - Q - f) \quad (5)$$

where $\text{SSQ}(\hat{\theta})$ is the residual sum of squares at the optimum solution, Q the number of parameters to be estimated, and f the degrees of freedom with pure error variance σ^2 .

For the model to fit adequately R must be smaller than the tabulated F -test values

$$R < F(M - Q - f, f) \quad (6)$$

The confidence intervals for the regression reaction rate parameters were calculated from

$$\frac{\text{SSQ}(\theta)}{\text{SSQ}(\hat{\theta})} = 1 + \frac{Q}{M - Q - f} F(M - Q - f, f) \quad (7)$$

where $\text{SSQ}(\theta)$ is the residual sum of squares some distance away from the optimum solution. All confidence intervals were calculated at a 95% significance level.

4. Results and Discussion

4.1. Experimental Results. The performance results obtained from the micro-fixed-bed reactor confirmed that the behavior of the coprecipitated cobalt–manganese oxide catalyst used is different from that of other cobalt-based catalysts. A publication by Keyser et al. (1998) gives a more detailed analysis of this catalyst and its catalytic behavior. The experimental results obtained in this investigation for different temperatures, pressures, volumetric flow rates, and feed compositions are given in Table 3. The results at each particular condition is the calculated average value involving at least three measurements. A significant yield of carbon dioxide was obtained as a result of the presence of the water–gas shift reaction, and the effects of the other operating parameters are consistent with previously published results for many other catalysts.

Table 3. Results Obtained with Co/MnO Catalyst [Co:Mn = 1:3 (by Mass)]

temperature (°C)	pressure (bar)	H ₂ :CO ratio (mol)	inlet flow rate [mL/min (STP)]	CO conversion (mol %) ^a	CO ₂ selectivity (mol %) ^b
210	11	1.90	22.0	9.96	3.16
220	26	1.65	22.0	29.4	2.7
220	21	1.65	22.0	24.0	3.6
220	16	1.65	22.0	21.0	4.1
220	11	1.65	22.0	18.0	4.6
220	11	1.90	39.9	9.45	2.85
220	6	1.65	22.0	13.1	5.9
220	26	4.05	22.0	45.4	1.8
220	16	4.05	22.0	38.0	1.9
220	6	4.05	22.0	24.2	2.3
230	11	1.90	22.0	22.2	7.00
230	11	1.90	39.9	9.0	4.6
240	11	1.90	22.0	34.9	8.9
240	11	1.90	39.9	18.09	6.9
250	11	1.90	22.0	43.2	14.7
250	11	1.90	43.3	26.3	10.3

^a CO conversion ($X_{\text{CO}} = 1 - u_{\text{CO}}/u^0 c_{\text{CO}}$). ^b CO₂ selectivity ($S_{\text{CO}_2} = [u_{\text{CO}_2} - u^0 c_{\text{CO}_2}]/[u^0 c_{\text{CO}} - u_{\text{CO}}]$).

4.2. Reaction Rates. For the determination of the most suitable reaction rate combination for the conversion of carbon monoxide and the production of the products (H₂, H₂O, CO₂, C_nH_m), all possible combinations of the Fischer–Tropsch and water–gas shift reaction rates given in Tables 1 and 2 were sequentially evaluated. Experimental results consisting of carbon monoxide conversions and the carbon dioxide concentrations given in Table 3 were used for the regression analysis. The number of data points varied between 24 and 40 for the different calculations. It should be noted that eq 6 which gives a measure of the goodness of fit takes into account the number of data points relative to the number of parameters (constants) to be estimated.

To ensure that the inclusion of the water–gas shift reaction was necessary, calculations were carried out with the Fischer–Tropsch equation only. None of the equations listed in Table 1 was found to agree with the experimental results. With the inclusion of the water–gas shift reactions (Table 2), it was also found necessary to include the pressure dependence (total pressure P) term to obtain agreement. A simple power dependence equation of the form P^d (d being some constant) was found to be suitable. Other investigators also found that the reaction rate was dependent on the total pressure and used a similar functional form as that used in this investigation (Attwood et al., 1950; Moe, 1962).

Results indicating the residual sum of squares and the goodness of fit according to eqs 4–6) obtained from the nonlinear calculation involving experimental results and predictions with the different reaction rate combinations at 220 °C are shown in Table 4. The values of the reaction parameters for the two best reaction rate combinations are shown in Table 5. It should be noted that the equation of Ledakowicz et al. (1989) gave results with the constant c equal to zero, thus reducing it to the equation of Anderson² (1956). The results in Tables 4 and 5 show that the Fischer–Tropsch reaction rate equations of Anderson² (1956) and Sarup and Wojciechowski (1989) are distinctly better than the other combinations for describing the overall kinetics of the reaction and that the measure of the goodness of fit is acceptable. The Anderson² (1956) equation which is based on the enolic theory is, however, marginally better than the Sarup and Wojciechowski (1989) equation based on the carbide theory. Hutchings et al. (1989)

Table 4. Results from Nonregression Calculations Involving Experimental Measurements and Predictable Results Using Reaction Rate Combinations at 220 °C

Fischer–Tropsch reaction rates (Table 1)	water–gas shift reaction rates (Table 2)			
	Singh and Saraf (1977)		Moe (1962)	
	residual sum of squares [SSQ]	goodness of fit (eqs 5 and 6)	residual sum of squares [SSQ]	goodness of fit (eqs 5 and 6)
Anderson ¹ (1956)	2.38	3.66 > $F(64,10) = 2.62$	2.12	3.24 > $F(64,10) = 2.62$
Rautavuoma and Van der Baan (1981)	7.94	12.58 > $F(64,10) = 2.62$	6.76	10.70 > $F(64,10) = 2.62$
Sarup and Wojciechowski (1989)	1.17	1.75 < $F(63,10) = 2.62$	3.14	4.96 > $F(63,10) = 2.62$
Yates and Satterfield (1991)	9.43	15.00 > $F(64,10) = 2.62$	10.98	17.48 > $F(64,10) = 2.62$
Huff and Sutterfield (1984)	5.95	9.39 > $F(64,10) = 2.62$	5.15	8.11 > $F(64,10) = 2.62$
Ledakowicz et al. (1984)	1.08	1.58 < $F(64,10) = 2.62$	9.83	15.64 > $F(64,10) = 2.62$
Anderson ² (1956)	1.08	1.58 < $F(64,10) = 2.62$	9.83	15.64 > $F(64,10) = 2.62$

Table 5. Reaction Rate Constants from Nonregression Calculation Involving the Two Most Successful Reaction Rate Combinations at 220 °C

	Anderson ² (1956) and Singh and Saraf (1977)	Sarup and Wojciechowski (1989) and Singh and Saraf (1977)
Fischer–Tropsch Reaction Rate Constants (Table 1)		
k_{FT}	$(6.399 \pm 0.778) \times 10^{-5}$	$(1.317 \pm 0.109) \times 10^{-4}$
b	10.30 ± 1.37	0.242 ± 0.025
c	—	0.185 ± 0.015
Water–Gas Shift Reaction Rate Constants (Table 2)		
k_{WGS}	$(1.057 \pm 0.049) \times 10^{-5}$	$(1.122 \pm 0.069) \times 10^{-5}$
P_f	$P^{0.69 \pm 0.05}$	$P^{0.75 \pm 0.05}$

Table 6. Results from Nonlinear Regression Calculation Involving the Fischer–Tropsch Reaction Rate of Anderson² (1956) and the Water–Gas Shift Reaction of Singh and Saraf (1977) over a Range of Temperatures (210–250 °C)

residual sum of squares (SSQ)	0.374
goodness of fit (R)	$0.89 < (32,10) > 2.70$
activation energies:	
Fischer–Tropsch reaction E_{FT}	79.9 ± 0.6 kJ/mol
water–gas shift reaction E_{WGS}	149.7 ± 0.3 kJ/mol

also found evidence that this reaction occurs through an enolic carbon species over a similar cobalt–manganese oxide catalyst. It is interesting to note that the Anderson² (1956) reaction rate equation was previously shown to be suitable for an iron-based catalyst, which means that the spinel-structured cobalt–manganese oxide catalyst used behaves very much like an iron-based catalyst in addition to having a water–gas shift reaction activity, in contrast to other cobalt-based catalysts. Many other investigators have used the Anderson² (1956) equation for iron-based catalysts, but none have used it successfully for cobalt-based catalysts.

The reaction rate combination consisting of the Fischer–Tropsch reaction of Anderson² (1956) and the water–gas shift reaction of Singh and Saraf (1977) was evaluated over a range of temperatures (210–250 °C) using Arrhenius-type equations for the temperature dependence of the reaction rate constants. The residual sum of squares, the goodness of fit, and the activation energies are shown in Table 6. It should be noted that the residual sum of squares and goodness of fit are better than the results obtained for the isothermal case (220 °C), which also confirms that the particular reaction rate combination is suitable for the other temperatures examined. The activation energy of 79.9 kJ/mol for the Fischer–Tropsch reaction compares very well with results quoted by Zimmerman and Bukur (1990). These authors summarized results obtained by other investigators with an equation similar to that of Anderson² (1956) and applicable to iron-based catalysts. Values of 85–89 kJ/mol have been reported. The activa-

tion energy shown in Table 6 for the water–gas shift reaction is higher than the value of 116 kJ/mol reported by Singh and Saraf (1977) for an iron-based catalyst.

5. Conclusions

The use of simultaneous reaction rate equations for the Fischer–Tropsch (hydrocarbon forming) and the water–gas shift reactions is considered essential for the successful modeling of the Fischer–Tropsch synthesis over a cobalt–manganese oxide catalyst. This was demonstrated with results from a fixed-bed reactor. A regression methodology consisting of the solution of reactor equations with simultaneous reaction rate equations was developed and tested. A reaction rate equation for the Fischer–Tropsch reaction based on the enolic mechanism gave results which were marginally better than results based on the carbide mechanism. The activation energy obtained for the cobalt–manganese oxide using the enolic-based equation is also very similar to the values reported in the literature for exclusively iron-based catalysts. It is concluded that the catalyst examined in this study also behaves very much like precipitated or fused iron catalysts. An empirical reaction rate equation for the simultaneous water–gas shift reaction using a first-order dependence was found to be suitable to account for the formation of carbon dioxide.

Acknowledgment

The authors are grateful to the management of Sastech research and development department, Sasol, South Africa, for the opportunity to have carried out this investigation and for permission to publish the results. M.J.K. is also grateful for the financial assistance obtained from the foundation for research development, FRD (South Africa).

Nomenclature

- a, b, c = temperature-dependent adsorption coefficients (Table 1)
 c_i = concentration of component i (mol/m³)
 d = pressure power dependence (constant)
 E_{FT} = Fischer–Tropsch reaction rate activation energy (kJ/mol)
 E_{WGS} = water–gas shift reaction activation energy (kJ/mol)
 f = degrees of freedom (eqs 5–7)
 F = F -test values
 k_{FT} = Fischer–Tropsch reaction rate constant (Table 1), mol/g·s·bar^(x)
 k_{WGS} = water–gas shift reaction rate constant (Table 2), mol/g·s·bar^(y)

K_{WGS} = water–gas shift reaction equilibrium constant
 m = average number of hydrogen atoms per hydrocarbon molecules
 M = number of experiments (eq 4)
 n = average carbon chain length of hydrocarbon
 N = number of chemical components (eq 4)
 p_i = partial pressure of component i (kPa)
 P = total pressure (kPa)
 P_f and P_r = pressure factor (Table 2), bar^d
 Q = number of parameters to be estimated (eqs 5–7)
 r_i = overall reaction rate of component i (mol/kg_{cat}·s)
 r_{FT} = reaction rate of the Fischer–Tropsch reaction (mol/kg_{cat}·s)
 r_{WGS} = reaction rate of the water–gas shift reaction (mol/kg_{cat}·s)
 r_{CO} = reaction rate for the formation of carbon monoxide (mol/kg_{cat}·s)
 R = parameter for measure of goodness of fit defined by eq 5
 S_i = selectivity of component i
 SSQ = residual sum of squares
 $\text{SSQ}(\theta)$ = residual sum of squares away from the optimum solution (eq 7)
 $\text{SSQ}(\hat{\theta})$ = residual sum of squares at the optimum solution (eqs 5 and 7)
 u = superficial velocity (m/s)
 x_{ij} = experimental variables, eq 4
 \hat{x}_{ij} = calculated variables, eq 4
 X_i = conversion of component i
 y_i = mole fraction of component i
 y_i^* = equilibrium mole fraction of component i
 z = axial coordinate (m)

Greek Symbols

σ^2 = error variance
 ρ_B = catalyst bed density (kg_{cat}/m³)

Super- and Subscripts

FT = Fischer–Tropsch
 i = index indicating components
 j = index indicating experiments
 $^\circ$ = reactor inlet
 WGS = water–gas shift

Literature Cited

- (1) Anderson, R. B. Catalysts for the Fischer–Tropsch Synthesis. In *Catalysis*; Emmett, P. H., Ed.; Van Nostrand-Reinhold: New York, 1956; Vol. IV.
- (2) Attwood, H. E.; Bennett, C. O. Kinetics of the Fischer–Tropsch reaction over iron. *Ind. Eng. Chem. Proc. Des. Dev.* **1979**, *18*, 163.
- (3) Attwood, K.; Arnold, M. R.; Appel, E. G. Water–gas shift reaction: effect of pressure on rate over an Fe oxide–Cr oxide catalyst. *Ind. Eng. Chem.* **1950**, *42*, 1600.
- (4) Blanks, R. F. Fischer–Tropsch synthesis gas conversion reactor. *Chem. Eng. Sci.* **1992**, *47* (5), 959.
- (5) Bohlbro, H. Kinetics of the water–gas conversion. IV. Influence of alkali in the rate equation. *J. Catal.* **1964**, *3*, 207.
- (6) Brown, K. M.; Dennis, J. E. Derivative free analogies of the Levenberg–Marquardt and Gauss algorithms for Nonlinear least squares approximation. *Numer. Math.* **1972**, *18*, 289.
- (7) Chanenchuk, C. A.; Yates, I. C.; Satterfield, C. N. The Fischer–Tropsch synthesis with a mechanical mixture of a cobalt catalyst and a copper-based water–gas shift catalyst. *Energy Fuels* **1991**, *5*, 847.
- (8) Deckwer, W. D.; Serpemen, Y.; Ralek, M.; Schmidt, B. Fischer–Tropsch synthesis in a slurry phase on Mn/Fe catalysts. *Ind. Eng. Chem. Process Des. Dev.* **1982**, *21*, 222.
- (9) Deluzarche, A.; Hindermann, J. P.; Kieffer, R.; Cressly, J.; Kiennemann, A. Mechanism of Fischer–Tropsch reactions in heterogeneous catalysis. *Bull. Soc. Chim. Fr.* **1982**, *17*, 171.
- (10) Draper, N. D.; Smith, H. *Applied regression analysis*, 2nd ed.; Wiley: New York, 1990.
- (11) Dry, M. E. Advances in Fischer–Tropsch chemistry. *Ind. Eng. Chem. Prod. Res. Dev.* **1976**, *15* (4), 282.
- (12) Everson, R. C.; Mulder, H.; Keyser, M. J. The Fischer–Tropsch reaction with supported ruthenium catalysts: Modelling and evaluation of the reaction rate equation for a fixed bed reactor. *Appl. Catal. A* **1996**, *142* (2), 223.
- (13) Finlayson, B. A. Packed-bed reactor analysis by orthogonal collocation. *Chem. Eng. Sci.* **1971**, *26*, 1081.
- (14) Froment, G. F.; Bischoff, K. B. *Chemical reactor analysis and design*, 2nd ed.; Wiley: New York, 1990.
- (15) Grenoble, D. C.; Edstadt, M. M.; Ollis, D. F. The chemistry and catalysis of the water–gas shift reaction. *J. Catal.* **1981**, *67*, 90.
- (16) Huff, G. A.; Satterfield, C. N. Intrinsic kinetics of the Fischer–Tropsch synthesis on a reduced fused magnetite catalyst. *Ind. Eng. Chem. Process Des. Dev.* **1984**, *23* (4), 696.
- (17) Hutchings, G. J.; Van der Riet, M.; Hunter, R. Carbon monoxide hydrogenation using cobalt/manganese oxide catalysts. *J. Chem. Soc., Faraday Trans. 1* **1989**, *85* (9), 2875.
- (18) Hutchings, G. J.; Copperthwaite, R.-E.; Gottschalk, F. M.; Hunter, R.; Mellor, J.; Orchard, W. S.; Sangiorgio, T. A comparative evaluation of cobalt chromium oxide, cobalt manganese oxide and copper manganese oxide as catalysts for the water–gas shift reaction. *J. Catal.* **1992**, *137*, 408.
- (19) Iglesia, E.; Reyes, S. C.; Madon, R. J.; Soled, S. I. Selectivity control and catalyst design in Fischer–Tropsch synthesis: sites, pellets and reactors. *Adv. Catal. Relat. Subj.* **1993**, *39*, 221.
- (20) Keyser, M. J. Kinetic study and reactor modelling of the Fischer–Tropsch synthesis with cobalt/manganese oxide catalyst. Ph.D. Thesis, Potchefstroom University for Christian Higher Education, Potchefstroom, South Africa, 1997.
- (21) Keyser, M. J.; Everson, R. C.; Espinoza, R. L. Fischer–Tropsch studies with cobalt manganese oxide catalysts: Synthesis performance in a fixed bed reactor. *Appl. Catal. A* **1998**, *171*, 99.
- (22) Ledakowicz, S.; Nettelhoff, H.; Kokuun, R.; Deckwer, W. D. Kinetics of the Fischer–Tropsch synthesis in the slurry phase on a potassium promoted iron catalyst. *Ind. Eng. Chem. Process Des. Dev.* **1985**, *24* (4), 1043.
- (23) Lox, E. S.; Froment, G. F. Kinetics of the Fischer–Tropsch reaction on a precipitated promoted iron catalyst. 2. Kinetic modelling. *Ind. Eng. Chem. Res.* **1993**, *32*, 71.
- (24) Mears, D. E. Diagnostic criteria for heat transport limitations in fixed bed reactors. *J. Catal.* **1971**, *20*, 127.
- (25) Moe, J. M. Design of water–gas shift reactors. *Chem. Eng. Prog.* **1962**, *58* (3), 33.
- (26) Nettlehoff, H. R.; Kokuun, R.; Ledakowicz, S.; Deckwer, W. D. Studies on the kinetics of Fischer–Tropsch synthesis in slurry phase. *Ger. Chem. Eng.* **1985**, *8*, 177.
- (27) Newsome, D. S. The water–gas shift reaction. *Catal. Rev. Sci. Eng.* **1980**, *21* (2), 275.
- (28) Oki, S.; Mezaki, R. Identification of rate controlling steps for the water–gas shift reaction over an iron catalyst. *J. Phys. Chem.* **1973a**, *77*, 447.
- (29) Oki, S.; Mezaki, R. Mechanistic structure of the water–gas shift reaction in the vicinity of chemical equilibrium. *J. Phys. Chem.* **1973b**, *77*, 1601.
- (30) Overstreet, A. D. A screening study of a new water–gas shift catalyst. M.S. Dissertation, Virginia Polytechnic Institute and State University, Blacksburg, VA, 1974.
- (31) Rautavuoma, A. O. I.; Van der Baan, H. S. Kinetics and mechanism of the Fischer–Tropsch hydrocarbon synthesis on a cobalt and alumina catalyst. *Appl. Catal.* **1981**, *1*, 247.
- (32) Ruthven, D. M. Activity of commercial water–gas shift catalysts. *Can. J. Chem. Eng.* **1969**, *47*, 327.
- (33) Sarup, B.; Wojciechowski, B. W. Studies of the Fischer–Tropsch synthesis on a cobalt catalyst. II. Kinetics of carbon monoxide conversion to methane and to higher hydrocarbons. *Can. J. Chem. Eng.* **1989**, *67*, 62.
- (34) Singh, C. P. P.; Saraf, D. N. Simulation of high-temperature water–gas shift reactors. *Ind. Eng. Chem. Process Des. Dev.* **1977**, *16* (3), 313.

(35) Yang, C. H.; Massoth, F. E.; Oblad, A. G. Kinetics of carbon monoxide and hydrogen reaction over cobalt–copper–aluminium oxide catalysts. *Adv. Chem. Ser.* **1979**, 178, 35.

(36) Yates, I. C.; Satterfield, C. N. Intrinsic kinetics of the Fischer–Tropsch synthesis on a cobalt catalyst. *Energy Fuels* **1991**, 5, 168.

(37) Young, I. C.; Finlayson, B. A. Axial dispersion in nonisothermal packed bed chemical reactors. *Ind. Eng. Chem. Fundam.* **1973**, 12 (4), 412.

(38) Zimmerman, W. H.; Bukur, D. B. Reaction kinetics over iron catalysts used for the Fischer–Tropsch synthesis. *Can. J. Chem. Eng.* **1990**, 68, 292.

Received for review March 30, 1999

Revised manuscript received September 17, 1999

Accepted October 11, 1999

IE990236F